

# Modified laminar flamelet presumed probability density function for LES of premixed turbulent combustion

M. Mahdi Salehi<sup>a,\*</sup>, W. Kendal Bushe<sup>a</sup>, Nasim Shahbazian<sup>b</sup>,  
Clinton P.T. Groth<sup>b</sup>

<sup>a</sup> Department of Mechanical Engineering, University of British Columbia, 6250 Applied Science Lane, Vancouver, BC, Canada V6T 1Z4

<sup>b</sup> Institute for Aerospace Studies, University of Toronto, 4925 Dufferin Street, Toronto, Ontario, Canada M3H 5T6

Available online 29 August 2012

## Abstract

The performance of the modified laminar flamelet probability density function (MLF-PDF) is studied as a presumed PDF for the PCM-FPI combustion model in LES. PCM-FPI is a low-cost flamelet model for turbulence–chemistry interactions in premixed and partially-premixed flames. The MLF-PDF couples the FPI tabulated detailed chemistry model with large eddy simulation. The performance of this PDF was examined before in an *a priori* analysis with DNS data [13] and in RANS simulations of laboratory-scale burners [14]. In this work, this PDF is first compared to the actual experimental PDF. Then it is demonstrated that the MLF-PDF recovers the filtered laminar flame speed which is an important factor when turbulence scales are larger than the flame thickness and are mostly resolved in the grid scale. Finally, this PDF is used in LES of a turbulent premixed bunsen flame. The mean radial distributions of temperature, a few major species and two radical species mass fractions are compared with experimental data. The results show that this new PDF is a viable option for the statistics of sub-grid scale progress variable fluctuations. © 2012 The Combustion Institute. Published by Elsevier Inc. All rights reserved.

**Keywords:** Presumed PDF; Turbulent premixed flames; PCM-FPI; LES

## 1. Introduction and background

In large eddy simulation (LES) of turbulent reacting flows, the rate-controlling processes – particularly most chemical reactions – happen at unresolved scales. As a result, turbulent combustion modelling in LES is still a modelling challenge. A variety of combustion models have been

proposed for LES of turbulent premixed flames. Apart from the linear eddy model, other LES combustion models have generally been adopted from similar RANS models [1]. For turbulent flames in the flamelet regime, several flamelet models are available in either the progress variable or *G*-equation form. Presumed conditional moments (PCM) [2] and flame surface density (FSD) models [3] utilize a transport equation for filtered progress variable to characterize the state of combustion. *G*-equation models are based on solving a transport equation for a filtered level set function *G* [4].

\* Corresponding author. Fax: +1 604 822 2403.

E-mail address: [salehima@interchange.ubc.ca](mailto:salehima@interchange.ubc.ca) (M. Mahdi Salehi).

The transported PDF model [5] and conditional moment closure (CMC) [6] are combustion models that are not limited to the flamelet regime. However, they are computationally expensive compared to the flamelet models and have their own modelling challenges. Givi [7] extended the transported PDF model from RANS to a combustion model for LES by introducing the idea of a filtered density function (FDF). The first LES combustion model based on the CMC hypothesis was proposed by Bushe and Steiner [8]. The transported PDF model has been extended to LES of premixed combustion [9] while the CMC has not yet been used as a combustion model for LES of premixed flames.

Flamelet models are easier to implement and computationally less expensive compared to transported PDF and CMC combustion models. The performance of flamelet models is satisfactory in the flamelet regime – an important practical regime, particularly for premixed flames. Hence, different variants of flamelet models have been used in commercial and academic simulation tools. In this work the presumed conditional moments (PCM) combustion model is used [2,10]. This model is predominantly used in combination with a flame prolongation of intrinsic low dimensional manifold (FPI) [11] or flamelet generated manifold (FGM) [12]. The model requires a presumed probability density function (PDF) of reaction progress variable for coupling between turbulence and chemistry. The modified laminar flamelet PDF (MLF-PDF) has proved to be a better presumed PDF model compared to the widely-used  $\beta$ -PDF in an *a priori* analysis using DNS data [13] and in RANS simulation of a laboratory-scale burner [14]. In this work, the MLF-PDF and the  $\beta$ -PDF are used in large eddy simulation of a turbulent premixed Bunsen burner and the results are compared with experiments. Also, it is demonstrated that this new PDF better represents the actual experimental PDF compared to the  $\beta$ -PDF.

## 2. Formulation

In large eddy simulation the three-dimensional unsteady large scale features of the flow field are captured and the small scales are filtered. Defining  $G(\mathbf{x})$  as a spatially-invariant low-pass filter function, the resolved portion of every quantity  $\phi$  can be expressed as:

$$\bar{\phi}(\mathbf{x}, t) = \int_V \phi(\mathbf{x}', t) G(\mathbf{x} - \mathbf{x}') d\mathbf{x}' \quad (1)$$

where  $\bar{\phi}$  is the filtered quantity. A density-weighting or Favre-filtering can also be defined as  $\bar{\phi} = \overline{\rho\phi}/\bar{\rho}$ . The transport equations for the large scale quantities can be obtained by applying the

above filtering operation to the governing equations of a reacting flow. The filtered conservation equation for mass fraction of species  $k$  assuming constant diffusivity is as follows:

$$\frac{\partial}{\partial t}(\bar{\rho}\tilde{Y}_k) + \frac{\partial}{\partial x_i}(\bar{\rho}\tilde{u}_i\tilde{Y}_k) = \frac{\partial}{\partial x_i}\left(\bar{\rho}\mathcal{D}\frac{\partial\tilde{Y}_k}{\partial x_i}\right) - \frac{\partial\tilde{\tau}_k}{\partial x_i} + \bar{\omega}_k \quad (2)$$

where,  $\bar{\rho}$  is the filtered mixture density,  $\tilde{Y}_k$  is the mass fraction of species  $k$ ,  $t$  is time,  $x_i$  is the spatial coordinate in  $i$ -direction,  $\tilde{u}_i$  is the filtered velocity in  $i$ -direction,  $\mathcal{D}$  is the molecular diffusivity,  $\tilde{\tau}_k = \bar{\rho}(\tilde{u}_i\tilde{Y}_k - \tilde{u}_i\tilde{Y}_k)$  is the unresolved turbulent scalar flux and  $\bar{\omega}_k$  is the filtered chemical reaction source term. The filtered chemical reaction source term is the result of interactions between chemical reactions and the sub-grid scale turbulence fluctuations. This interaction in the PCM-FPI flamelet model is reflected through a model for the filtered probability density function (also known as FDF [7]) of a reaction progress variable. The filtered PDF of reaction progress variable  $c(\mathbf{x}, t)$  is defined as [15]:

$$\bar{P}(c^*; \mathbf{x}, t) \equiv \int_V \delta[c^* - c(\mathbf{x}', t)] G(\mathbf{x} - \mathbf{x}') d\mathbf{x}' \quad (3)$$

where  $\delta$  is the Dirac delta function. The conditional filtered value of every quantity  $\phi(\mathbf{x}, t)$  can also be defined knowing the PDF:

$$\overline{\phi(\mathbf{x}, t)|c^*} \equiv \frac{\int_V \phi(\mathbf{x}', t) \delta[c^* - c(\mathbf{x}', t)] G(\mathbf{x} - \mathbf{x}') d\mathbf{x}'}{\bar{P}(c^*; \mathbf{x}, t)} \quad (4)$$

If the above equation is expressed for the chemical reaction source term and is integrated in the progress variable space, the following expression is obtained:

$$\bar{\omega}_k(\mathbf{x}, t) = \int_0^1 \overline{\omega}_k(\mathbf{x}, t)|c^* \bar{P}(c^*; \mathbf{x}, t) dc^* \quad (5)$$

In the PCM-FPI combustion model the conditional averages are assumed to be the laminar flamelet values. These values come from the FPI chemistry model. In the FPI chemistry model an unstrained steady one-dimensional laminar premixed flame is obtained using detailed chemistry. The chemical reaction source terms and species mass fractions are then tabulated as a function of a progress variable  $c^* = Y_c/Y_c^{eq}$  where  $Y_c = Y_{CO_2} + Y_{CO}$  is chosen in this study [2]. The PCM-FPI combustion model requires a presumed functional form for the filtered PDF. This function is formed knowing the filtered progress variable  $\tilde{c}$  and sub-grid scale variance of the reaction progress variable  $\tilde{c}_v \equiv \tilde{c}c - \tilde{c}\tilde{c}$  at each point. This parameter can be normalized with maximum possible variance and is called segregation factor  $Sc = \tilde{c}_v/(\tilde{c}(1 - \tilde{c}))$ . Based on these assumptions

the chemical reaction source term at each point in space and time ( $\mathbf{x}, t$ ) is:

$$\overline{\dot{\omega}_k} \approx \int_0^1 \dot{\omega}_k(c^*) \text{FPI} \overline{P}(c^*; \tilde{c}, \tilde{c}_v) dc^* \quad (6)$$

The above integration can be done *a priori* and  $\overline{\dot{\omega}_k}$  can be stored in a table as a function of  $\tilde{c}$  and  $\tilde{c}_v$ .

2.1. Presumed PDF model

The  $\beta$ -function has been used as a PDF model for PCM-FPI combustion model [16,17]. However, this PDF is used primarily because it can recover the limits of extremely high and extremely low variance. While it has been used very successfully in non-premixed combustion, in premixed combustion, it over-predicts the progress variable chemical reaction source term and does not always give satisfactory results for premixed combustion [13,14,18–20].

Bray et al. proposed a laminar flamelet-based PDF:

$$\overline{P}(c^*) = A\delta(c^*) + \frac{B}{|\nabla c^*|} + C\delta(1 - c^*) \quad (7)$$

where  $|\nabla c^*|$  is calculated from an one-dimensional unstrained laminar premixed flame.  $A$ ,  $B$  and  $C$  are unknown constants that are calculated knowing the mean and variance of the progress variable and the constraint that  $\int_0^1 \overline{P}(c^*) dc^* = 1$ . This PDF is applicable only for relatively high variance values [14]. In order to overcome this limitation, Jin et al. [13] proposed dropping one  $\delta(c^*)$  and clipping the Bray PDF at  $c_1^* > 0$  or at  $c_2^* < 1$  or dropping both Dirac delta functions and clipping the Bray PDF at both  $c_1^* > 0$  and  $c_2^* < 1$ , depending on the variance and mean. Therefore, four different general shapes for the PDF become possible which cover the entire range of realizable values of mean and variance, as shown in Fig. 1. In each case three unknowns must be calculated from the mean, variance and the constraint that  $\int_0^1 \overline{P}(c^*) dc^* = 1$ . This modified PDF – called the modified laminar flamelet PDF (MLF-PDF) – is affected by changes to the chemical kinetic mechanism and how these affect the shape of the laminar premixed flame [13].

2.2. Presumed PDF models versus experimental PDF

The experimental data of Sweeney et al. [21] is available to generate PDFs of progress variable. In this experiment a lean turbulent premixed methane–air flame is formed in a slot burner at equivalence ratio of 0.73. Figure 3 compares the experimental PDF, MLF-PDF and the  $\beta$ -PDF at two different locations. This figure shows that the MLF-PDF is a better presumed PDF model compared to the  $\beta$ -PDF.

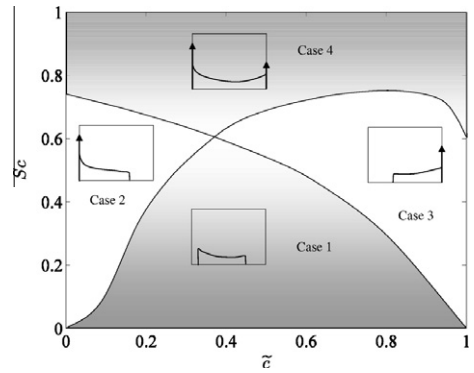


Fig. 1. Four possible shapes for the modified laminar flamelet PDF for lean methane–air premixed flame.  $Sc$  is the segregation factor  $Sc = \tilde{c}_v / (\tilde{c}(1 - \tilde{c}))$ .

2.3. Filtered laminar flame speed

Fiorina et al. [19] have studied the ability of the  $\beta$ -PDF to recover the filtered laminar flame speed. This is of particular importance when all the turbulence scales are captured in the grid scale and there is no sub-grid scale wrinkling. In this case, the filtered flame speed  $S_\Delta$  is equal to the laminar flame speed  $S_l$ . In a canonical case of a steady one-dimensional laminar premixed flame the following equation is valid:

$$\rho^u S_l \frac{dc}{d\xi} = \frac{d}{d\xi} \left( \rho D \frac{dc}{d\xi} \right) + \dot{\omega}_c(\xi) \quad (8)$$

where  $\rho^u$  is the density of unburned gases,  $\rho$  is the mixture density,  $c$  is the progress variable and  $\xi$  is the spatial coordinate. After filtering Eq. (8) with a Gaussian filter of size  $\Delta$  and integrating this equation and the filtered version, the following relation is valid [19]:

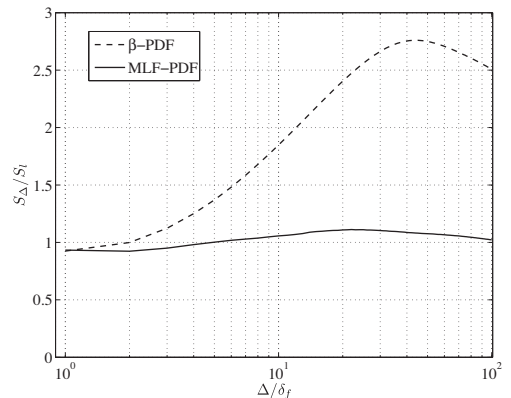


Fig. 2. Filtered laminar flame speed for different filter sizes using  $\beta$ -PDF and MLF-PDF.

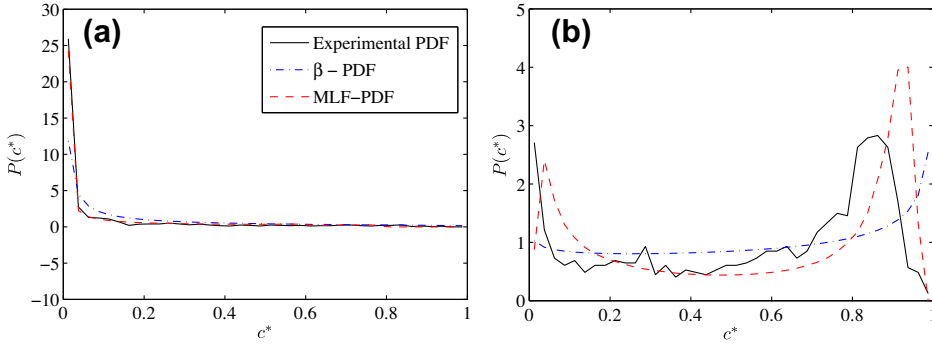


Fig. 3. Experimental and presumed PDFs of the progress variable. (a)  $\bar{c} = 0.03$  and  $\bar{c}_v = 0.01$ , (b)  $\bar{c} = 0.4$  and  $\bar{c}_v = 0.12$ .

$$\rho^u S_\Delta = \int_{-\infty}^{+\infty} \bar{\omega}_c(\xi) d\xi = \int_{-\infty}^{+\infty} \dot{\omega}_c(\xi) d\xi = \rho^u S_l \quad (9)$$

The filtered laminar flame speed  $S_\Delta$  can be calculated for different filter sizes  $\Delta$  using the  $\beta$ -PDF and the MLF-PDF. As pointed out in [19] the  $\beta$ -PDF does not satisfy Eq. (9). This is shown in Fig. 2. This figure also shows that the MLF-PDF satisfies Eq. (9) with relatively good accuracy, which suggests that the MLF-PDF ought to perform better in LES calculations of premixed turbulent flames in the flamelet regime.

#### 2.4. LES SGS closures

In the PCM-FPI combustion model, two transport equations for  $\tilde{c}$  and  $\tilde{c}_v$  are solved in addition to the continuity, momentum and energy equations. The transport equation for  $\tilde{c}$  is similar to Eq. (12). In this work a  $k$ -equation SGS model is used where one transport equation is solved for sub-grid scale turbulent kinetic energy [22]. The SGS turbulent kinetic energy is used to model the turbulent viscosity and the Reynolds stress tensor is obtained through the eddy-viscosity hypothesis. The unresolved turbulent scalar flux in Eq. (12) is closed using a gradient assumption:

$$\bar{\tau}_k = \bar{\rho}(\widetilde{u_i Y_k} - \widetilde{u_i} \widetilde{Y_k}) \approx -\rho \frac{v_T}{Sc_T} \frac{\partial \widetilde{Y_k}}{\partial x_i} \quad (10)$$

where  $Sc_T$  is a turbulent Schmidt number and  $v_T$  is the SGS turbulent viscosity. Equation (10) is not valid when counter-gradient diffusion occurs. However,  $\bar{\tau}_k$  is small in LES compared to RANS, because in LES the large scale portion of the turbulent scalar flux is captured. Also, as the grid resolution increases, the uncertainty in modelling this term decreases in LES [23]. Moreover, counter-gradient diffusion does not happen when the Bray number is less than one.

The transport equation for  $\tilde{c}_v$  after using the gradient diffusion assumption for unresolved scalar fluxes with a single Schmidt number is as follows [2]:

$$\begin{aligned} \frac{\partial}{\partial t} (\bar{\rho} \tilde{c}_v) + \frac{\partial}{\partial x_i} (\bar{\rho} \tilde{u}_i \tilde{c}_v) &= \frac{\partial}{\partial x_i} \left( \bar{\rho} D \frac{\partial \tilde{c}_v}{\partial x_i} \right) \\ &+ \frac{\partial}{\partial x_i} \left( \bar{\rho} \frac{v_T}{Sc_T} \frac{\partial \tilde{c}_v}{\partial x_i} \right) + 2\bar{\rho} \frac{v_T}{Sc_T} \frac{\partial \tilde{c}}{\partial x_i} \frac{\partial \tilde{c}}{\partial x_i} \\ &- 2\bar{s}_{\gamma_c} + 2(\bar{\omega}_c c - \bar{\omega}_c \tilde{c}) \end{aligned} \quad (11)$$

where  $\bar{\omega}_c$  is the filtered chemical reaction source term in the progress variable transport equation;  $\bar{\omega}_c c$  is also unclosed and is computed by integrating over the filtered PDF and stored;  $\bar{s}_{\gamma_c}$  is the SGS scalar dissipation rate and can be modelled using a linear relaxation:

$$\bar{s}_{\gamma_c} = \bar{\rho} \frac{v_T}{Sc_T} \frac{\tilde{c}_v}{\Delta^2} \quad (12)$$

where  $\Delta$  is the filter scale.

### 3. Implementation

The chemistry library was generated by solving a one-dimensional unstrained laminar premixed flame calculated with Cantera [24]. GRI-MECH 3.0 [25] detailed chemistry mechanism is used to obtain the chemistry library. Continuity, momentum and energy equations are solved along with a transport equation for the SGS turbulent kinetic energy. Two additional transport equations are solved for the filtered and SGS fluctuation of reaction progress variable. Species mass fractions are tracked by solving transport equations. The chemical reaction source-terms for species transport equations are reconstructed from the species mass fractions read in the PCM-FPI look-up table [10]. These transport equations are solved using a compressible density-based approach available in the CFFC code [26]. In this code, the temporal derivatives are solved using a second-order Runge–Kutta scheme and spatial derivatives are solved via a second-order finite volume approach. The inviscid fluxes are calculated using limited linear reconstruction and a Riemann-solver-based flux calculation approach. Viscous fluxes are

computed via a hybrid average gradient-diamond path. The details of the computational approach can be found in [26]. A multi-block hexahedral mesh is used and all the computations are done in parallel using a domain decomposition approach with MPI.

The premixed Bunsen flame of Chen et al. [27] is simulated in this work. In this burner the stoichiometric mixture of methane and air enters as a central cold jet at different Reynolds numbers. This central jet is surrounded by hot pilot products of a methane–air flame at the same equivalence ratio for stabilization. This geometry is modelled with over 1.6 million hexahedral computational cells and is run on 128 processors. Almost 93% of the turbulent kinetic energy is resolved on the grid scale. Also, the grid resolution in the reaction zone is between 2 and 10 times bigger than the unstrained laminar flame thickness. In this study flame F3 of this burner is simulated which has a mean inlet velocity of 30 m/s. The inlet velocity comes from a precursor LES simulation of a periodic pipe with  $L/D = 20$ . For this flame the Bray number is less than one [14]; hence, the gradient diffusion assumption should be valid.

#### 4. Results and discussion

The simulations are run with the initialization of a cylinder of reactants inside a domain otherwise filled with products. Each simulation is run until the total heat release in the domain achieves a statistically stationary condition. Statistics are collected thereafter. Figure 4 shows the instantaneous contours of density field for the turbulent premixed Bunsen flame.

The radial profiles of different mean quantities were measured in the experiments at four axial locations. Figure 5 shows the comparison between the experimental results and numerical predictions for mean temperature. Predictions at the lowest axial locations  $x/D = 2.5$  are affected by the uncertainty in the inlet boundary condition for the pilot stream. This figure shows that the  $\beta$ -PDF over-predicts the temperature due to over-estimation of the reaction rates and local over-heating. The deviations from experiment at farther downstream locations in both models are likely due to using a simple model for SGS turbulent kinetic energy. Using a dynamic model may improve the predictions.

Large-eddy simulation of this flame is also done by Knudsen and Pitsch [28], Yilmaz et al. [9] and Wang et al. [29]. The temperature results in [9,28] are slightly better than this work. A transported PDF combustion model is used in [9] which is a better approach compared to the simple flamelet model employed in this work. Knudsen and Pitsch [28] adjusted the inlet temperature to account for the uncertainty in the

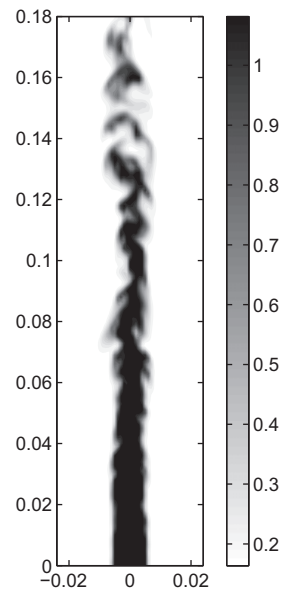


Fig. 4. Instantaneous contours of density for flame F3.

temperature inlet boundary condition. Also, they used a dynamic LES model which is better than  $k$ -equation model used in this work. The temperature results of Wang et al. [29] are not as good as the results shown in Fig. 5. This is likely due to using a single step, irreversible chemistry in [29].

Radial profiles of two major species mass fractions are shown in Figs. 6 and 7. These figures show that the performance of the  $\beta$ -PDF and the MLF-PDF in predicting the major species mass fractions are similar. In both case, the numerical predictions are close to experimental results. Other reported LES results [28,9,29] have similar performance in reproducing the experimental results for major species mass fractions.

Figure 8 shows the radial profiles of OH mass fraction, a radical species that is hard to predict. This figure shows that both PDFs under-estimate the OH mass fractions; however, the results of using the MLF-PDF are closer to the experimental results. Both methods have a reasonably good prediction of the CO mass fraction as shown in Fig. 9. This figure shows that the MLF-PDF provides a better prediction of the trend in the experimental results at farther downstream locations. At these locations the CO mass fraction increases, has a peak at  $r/D = 0.5$  and then decreases. The MLF-PDF captures this trend while in the  $\beta$ -PDF results the CO mass fractions remains constant up to  $r/D = 1.0$  before decreasing. Among other three large-eddy simulations of this burner, only Yilmaz et al. [9] reported OH and CO mass fractions. They have a better prediction for OH while CO results in this work are closer to experiment.

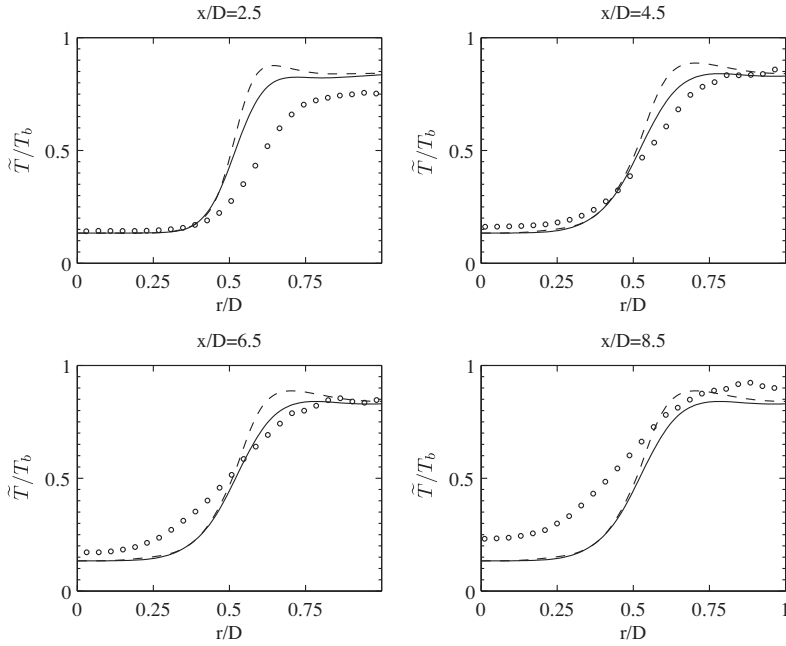


Fig. 5. Radial profiles of mean temperature at four different axial locations for turbulent Bunsen flame F3 [27]. Symbols denote experimental data, “- -” shows the simulation results using  $\beta$ -PDF and “—” is the result of using MLF-PDF.  $T_b$  is the adiabatic flame temperature.

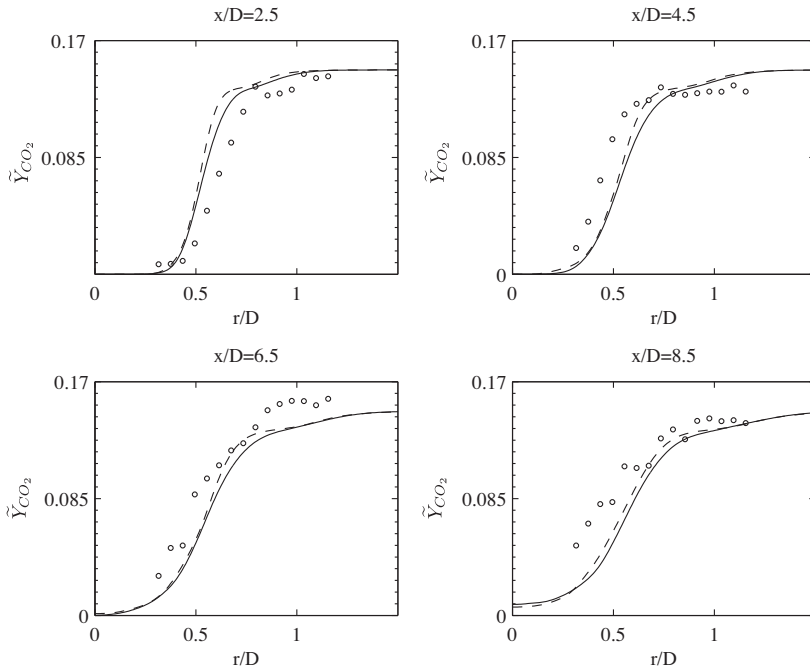


Fig. 6. Radial profiles of mean  $CO_2$  mass fraction at four different axial locations for turbulent Bunsen flame F3 [27]. Symbols denote experimental data, “- -” shows the simulation results using  $\beta$ -PDF and “—” is the result of using MLF-PDF.

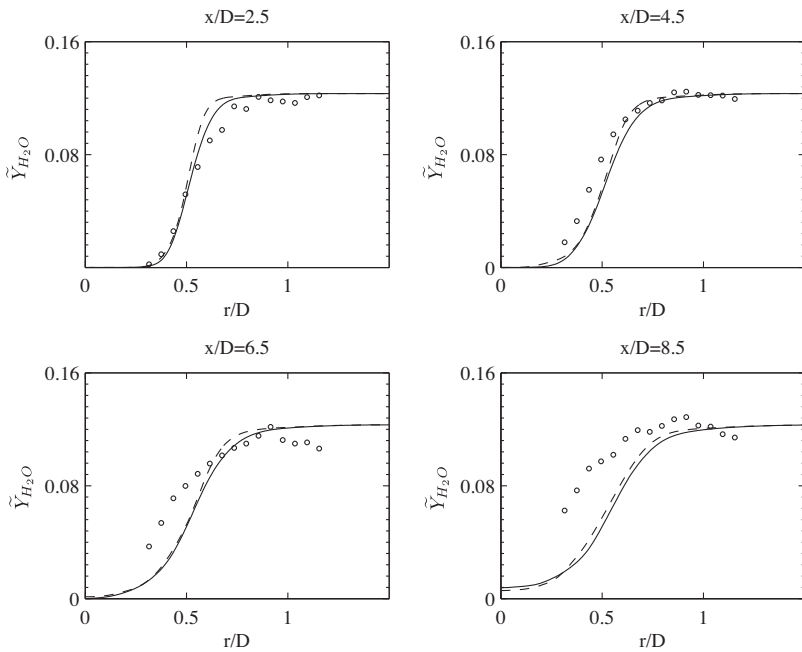


Fig. 7. Radial profiles of mean  $H_2O$  mass fraction at four different axial locations for turbulent Bunsen flame F3 [27]. Symbols denote experimental data, “- -” shows the simulation results using  $\beta$ -PDF and “—” is the result of using MLF-PDF.

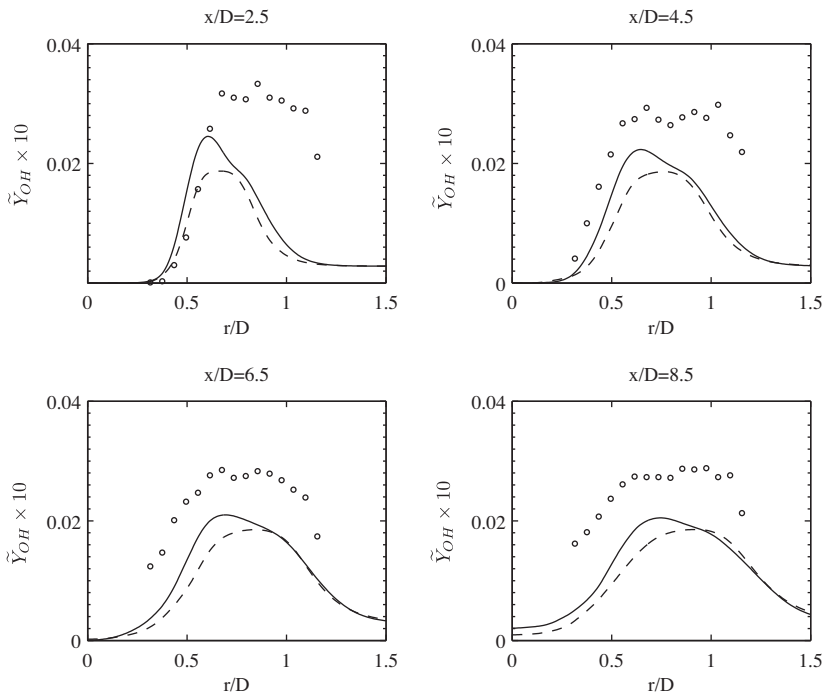


Fig. 8. Radial profiles of mean  $OH$  mass fraction at four different axial locations for turbulent Bunsen flame F3 [27]. Symbols denote experimental data, “- -” shows the simulation results using  $\beta$ -PDF and “—” is the result of using MLF-PDF.

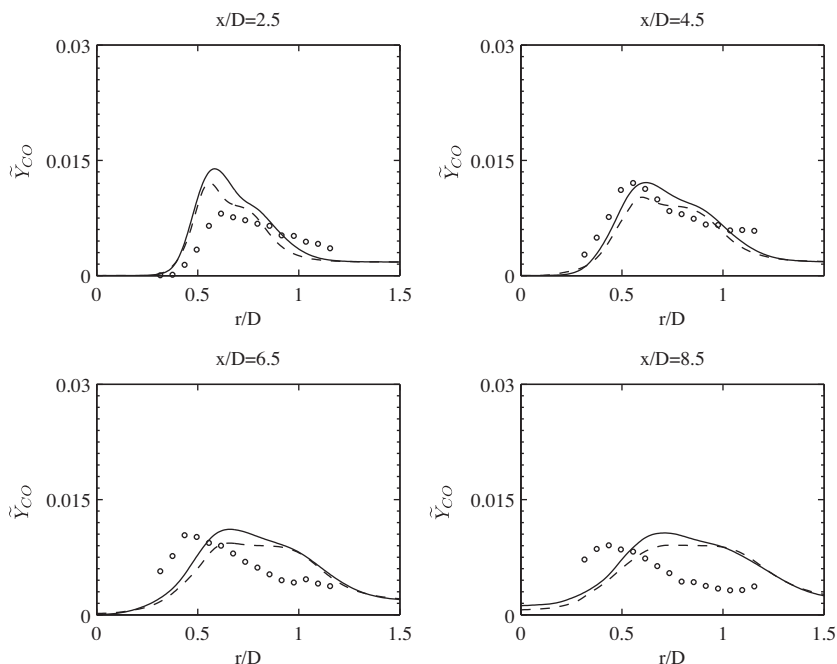


Fig. 9. Radial profiles of mean CO mass fraction at four different axial locations for turbulent Bunsen flame F3 [27]. Symbols denote experimental data, “- -” shows the simulation results using  $\beta$ -PDF and “—” is the result of using MLF-PDF.

Altogether, in this burner both the  $\beta$ -PDF and the MLF-PDF have good predictions of the species mass fractions, but the MLF-PDF results are slightly better. Unlike the  $\beta$ -PDF, the MLF-PDF is based on the chemistry and has a much better prediction of the filtered flame speed as shown in Section 2.3. Also, The MLF-PDF is more similar to the experimental PDF compared to the  $\beta$ -PDF. Therefore, the MLF-PDF is a better candidate for the statistical representation of the reaction progress variable.

## 5. Concluding remarks

PCM-FPI is a low-cost flamelet model for turbulence–chemistry interactions in a premixed flame. This model requires a presumed PDF model for the progress variable. In this work, the modified laminar flamelet PDF (MLF-PDF) is compared with the widely-used  $\beta$ -PDF. First, it is shown that the MLF-PDF better represent the actual experimental PDF as opposed to the  $\beta$ -PDF. Then, it is demonstrated that prediction of the filtered laminar flame speed using the MLF-PDF is superior to that obtained using the  $\beta$ -PDF. Both PDF models are then used in large-eddy simulation of a turbulent premixed laboratory-scale Bunsen flame. The results with the MLF-PDF are marginally better compared to those from the  $\beta$ -PDF. The only penalty in

using the MLF-PDF is associated with assembling the pre-calculated table, which must be re-done to account for any changes to the thermochemical properties of the flame, including changes to the chemistry or the composition or state of the reactant stream. Otherwise, the computational cost of using it in LES calculations is equal to that of using the  $\beta$ -PDF. Clearly, the MLF-PDF should be the preferred option for presumed PDF modelling of turbulent premixed flames.

## Acknowledgements

The authors acknowledge the financial support of MITACS and Rolls-Royce Canada. Computations were performed on the GPC supercomputer at the SciNet HPC Consortium. SciNet is funded by: the Canada Foundation for Innovation under the auspices of Compute Canada; the Government of Ontario; Ontario Research Fund – Research Excellence; and the University of Toronto.

## References

- [1] H. Pitsch, *Ann. Rev. Fluid Mech.* 38 (2006) 453–482.
- [2] P. Domingo, L. Vervisch, S. Payet, R. Hauguel, *Combust. Flame* 143 (4) (2005) 566–586.
- [3] E.R. Hawkes, R.S. Cant, *Proc. Combust. Inst.* 28 (2000) 51–58.

- [4] W.W. Kim, S. Menon, *Combust. Sci. Technol.* 160 (2000) 119–150.
- [5] S.B. Pope, *Prog. Energy Combust. Sci.* 11 (1985) 119–192.
- [6] A.Y. Klimenko, R.W. Bilger, *Prog. Energy Combust. Sci.* 25 (1999) 595–687.
- [7] P. Givi, *Prog. Energy Combust. Sci.* 15 (1989) 1–107.
- [8] W.K. Bushe, H. Steiner, *Phys. Fluids* 11 (7) (1999) 1896–1906.
- [9] S.L. Yilmaz, M.B. Nik, P. Givi, P.A. Strakey, *J. Prop. Power* 26 (1) (2010) 84–93.
- [10] J. Galphin, A. Naudin, L. Vervisch, C. Angelberger, O. Colin, P. Domingo, *Combust. Flame* 155 (2008) 247–266.
- [11] O. Gicquel, N. Darabiha, D. Thévenin, *Proc. Combust. Inst.* 28 (2000) 1901–1908.
- [12] J.A. van Oijen, F.A. Lammers, L.P.H. de Goeij, *Combust. Flame* 127 (3) (2001) 2124–2134.
- [13] B. Jin, R. Grout, W.K. Bushe, *Flow Turbul. Combust.* 81 (4) (2008) 563–582.
- [14] M.M. Salehi, W.K. Bushe, *Combust. Theory Model.* 14 (3) (2010) 381–403.
- [15] P.J. Colucci, F.A. Jaber, P. Givi, S.B. Pope, *Phys. Fluids* 10 (2) (1998) 499–515.
- [16] B. Fiorina, O. Gicquel, L. Vervisch, S. Carpentier, N. Darabiha, *Proc. Combust. Inst.* 30 (2005) 867–874.
- [17] F.E. Hernandez-Perez, F.T.C. Yuen, C.P.T. Groth, O.L. Gulder, *Proc. Combust. Inst.* 33 (2011) 1365–1371.
- [18] K.N.C. Bray, M. Champion, P.A. Libby, N. Swaminathan, *Combust. Flame* 146 (4) (2006) 665–673.
- [19] B. Fiorina, R. Vicquelin, P. Auzillon, N. Darabiha, O. Gicquel, D. Veynante, *Combust. Flame* 157 (3) (2010) 465–475.
- [20] G. Lecocq, S. Richard, O. Colin, L. Vervisch, *Combust. Flame* 158 (6) (2011) 1201–1214.
- [21] M.S. Sweeney, S. Hochgreb, R.S. Barlow, *Combust. Flame* 158 (5) (2011) 935–948.
- [22] A. Yoshizawa, K. Horiuti, *J. Phys. Soc. Jpn.* 54 (8) (1985) 2834–2839.
- [23] T. Poinsot, D. Veynante, *Theoretical and Numerical Combustion*, R.T. Edwards Inc., Philadelphia, 2001.
- [24] D.G. Goodwin, Cantera: Object-Oriented Software for Reacting Flows, available at <<http://www.cantera.org>>.
- [25] G.P. Smith et al., GRI-MECH 3.0, available at <[http://www.me.berkeley.edu/gri\\_mech/](http://www.me.berkeley.edu/gri_mech/)>.
- [26] X. Gao, C.P.T. Groth, *J. Comput. Phys.* 229 (9) (2010) 3250–3275.
- [27] Y.C. Chen, N. Peters, G.A. Schneemann, N. Wruck, U. Renz, M.S. Mansour, *Combust. Flame* 107 (3) (1996) 223–244.
- [28] E. Knudsen, H. Pitsch, *Combust. Flame* 154 (4) (2008) 740–760.
- [29] G. Wang, M. Boileau, D. Veynante, *Combust. Flame* 158 (11) (2011) 2199–2213.